

Stick Graphs with Length Constraints[∗]

Steven Chaplick, Philipp Kindermann, Andre Löffler, Florian Thiele,
Alexander Wolff, Alexander Zaft, and Johannes Zink

Institut für Informatik, Universität Würzburg, Würzburg, Germany
 firstname.lastname@uni-wuerzburg.de

Abstract. Stick graphs are intersection graphs of horizontal and vertical line segments that all touch a line of slope -1 and lie above this line. De Luca et al. [GD’18] considered the recognition problem of stick graphs when no order is given (**STICK**), when the order of either one of the two sets is given (**STICK_A**), and when the order of both sets is given (**STICK_{AB}**). They showed how to solve **STICK_{AB}** efficiently.

In this paper, we improve the running time of their algorithm, and we solve **STICK_A** efficiently. Further, we consider variants of these problems where the lengths of the sticks are given as input. We show that these variants of **STICK**, **STICK_A**, and **STICK_{AB}** are all NP-complete. On the positive side, we give an efficient solution for **STICK_{AB}** with fixed stick lengths if there are no isolated vertices.

1 Introduction

For a given collection \mathcal{S} of geometric objects, the *intersection graph* of \mathcal{S} has \mathcal{S} as its vertex set and an edge whenever $S \cap S' \neq \emptyset$, for $S, S' \in \mathcal{S}$. This paper concerns *recognition* problems for classes of intersection graphs of restricted geometric objects, i.e., determining whether a given graph is an intersection graph of a family of restricted sets of geometric objects. A classic (general) class of intersection graphs is that of *segment graphs*, the intersection graphs of line segments in the plane¹. For example, segment graphs are known to include planar graphs [4]. The recognition problem for segment graphs is $\exists\mathbb{R}$ -complete [18,22]². On the other hand, one of the simplest natural subclasses of segment graphs is that of the *permutation graphs*, the intersection graphs of line segments where there are two parallel lines such that each line segment has its two end points on these parallel lines³, we say that the segments are *grounded* on these two lines. The recognition problem for permutation graphs can be solved in linear time [19]. *Bipartite* permutation graphs have an even simpler intersection representation [25]: they

[∗] S.C. and A.W. acknowledge support from DFG grants WO 758/11-1 and WO 758/9-1.

¹ We follow the common convention that parallel segments do not intersect and each point in the plane belongs to at most two segments.

² Note that $\exists\mathbb{R}$ includes NP, see [22,24] for background on the complexity class $\exists\mathbb{R}$.

³ i.e., we think of the sequence of end points on the “bottom” line as one permutation π on the vertices and the sequence on the top line as another permutation π' , where uv is an edge if and only if the order of u and v differs in π and π' .

are the intersection graphs of unit-length vertical and horizontal line segments which are again double-grounded (without loss of generality both lines have a slope of -1). The simplicity of bipartite permutation graphs leads to a simpler linear-time recognition algorithm [27] than that of permutation graphs.

Several recent articles [1,2,6,7] compare and study the geometric intersection graph classes occurring between the simple classes, such as bipartite permutation graphs, and the general classes, such as segment graphs. Cabello and Ježić [1] mention that studying such classes with constraints on the sizes or lengths of the objects is an interesting direction for future work (and such constraints are the focus of our work). Note that similar length restrictions have been considered for other geometric intersection graphs such as interval graphs [15,16,23].

When the segments are not grounded, but still are only horizontal and vertical, the class is referred to as *grid intersection graphs* and it also has a rich history, see, e.g., [6,7,13,17]. In particular, note that the recognition problem is NP-complete for grid intersection graphs [17]. But, if both the permutation of the vertical segments and the permutation of the horizontal segments are given, then the problem becomes a trivial check on the bipartite adjacency matrix [17]. However, for the variant where only one such permutation, e.g., the order of the horizontal segments, is given, the complexity remains open. A few special cases of this problem have been solved efficiently [5,9,10], e.g., one such case [5] is equivalent to the problem of *level planarity testing* which can be solved in linear time [14].

In this paper we study recognition problems concerning so-called *stick* graphs, the intersection graphs of grounded vertical and horizontal line segments (i.e., grounded grid intersection graphs). Classes closely related to stick graphs appear in several application contexts, e.g., in *nano PLA-design* [26] and detecting *loss of heterozygosity events in the human genome* [3,12]. Note that, similar to the general case of segment graphs, it was recently shown that the recognition problem for grounded segments (where arbitrary slopes are allowed) is $\exists\mathbb{R}$ -complete [2]. So, it seems likely that the recognition problem for stick graphs is NP-complete (similar to grid intersection graphs), but thus far it remains open. The primary prior work on recognizing stick graphs is due to De Luca et al. [9]. Similarly to Kratochvíl's approach to grid intersection graphs [17], De Luca et al. characterized stick graphs through their bipartite adjacency matrix and used this result as a basis to develop polynomial-time algorithms to solve two constrained cases of the stick graph recognition problem called STICK_A and STICK_{AB} , defined next. However, their algorithm for STICK_A is incorrect [21], leaving STICK_A open.

Definition 1 (STICK). Let G be a bipartite graph with vertex set $A \cup B$, and let ℓ be a line with slope -1 . Decide whether G has an intersection representation where the vertices in A are vertical line segments whose bottom end-points lie on ℓ and the vertices in B are horizontal line segments whose left end-points lie on ℓ .⁴ Such a representation is a stick representation of G , the line ℓ is the ground line, the segments are called sticks, and the point where a stick meets ℓ is its foot point.

⁴ Note that De Luca et al. [9] regarded A as horizontal segments.

Table 1: Previously known and new results for deciding whether a given bipartite graph $G = (A \cup B, E)$ is a stick graph. In $O(\cdot)$, we dropped $|\cdot|$. NPC means NP-complete.

given order	variable length		fixed length		
	old	new	isolated vertices	no isolated vertices	
\emptyset	unknown	unknown	NPC [Thm. 3]	NPC	[Thm. 3]
A	unknown	$O(AB)$ [Thm. 2]	NPC [Thm. 4]	NPC	[Thm. 4]
A, B	$O(AB)$ [9]	$O(E)$ [Thm. 1]	NPC [Cor. 2]	$O((A+B)^2)$	[Cor. 3]

Definition 2 (STICK_A/STICK_{AB}). In the problem STICK_A (STICK_{AB}) we are given an instance of the STICK problem and additionally an order σ_A (orders σ_A, σ_B) of the vertices in A (in A and B). The task is to decide whether there is a stick representation that respects σ_A (σ_A and σ_B).

Our Contribution. We first revisit the problems STICK_A and STICK_{AB} defined by De Luca et al. [9]. We provide the first efficient algorithm for STICK_A and a faster algorithm for STICK_{AB}; see Section 2. Then we investigate the direction suggested by Cabello and Jejčić [1] where specific lengths are given for the segments of each vertex. In particular, this can be thought of as generalizing from unit stick graphs (i.e., bipartite permutation graphs), where every segment has the same length. While bipartite permutation graphs can be recognized in linear time [27], it turns out that all of the new problem variants (which we call STICK^{fix}, STICK_A^{fix}, and STICK_{AB}^{fix}) are NP-complete; see Section 3. Finally, we give an efficient solution for STICK_{AB}^{fix} (that is, STICK_{AB} with fixed stick lengths) for the special case that there are no isolated vertices (see Section 3.3). We conclude and state some open problems in Section 4. Our results are summarized in Table 1.

2 Sticks of Variable Lengths

In this section, we provide algorithms for the STICK_A problem in $O(|A||B|)$ time (Theorem 2) and the STICK_{AB} problem in $O(|A| + |B| + |E|)$ time (Theorem 1). Both algorithms apply a sweep-line approach (with a vertical sweep-line moving rightwards) where each vertical stick $a_i \in A$ corresponds to two events: the *enter event of a_i* (abbreviated by i) and the *exit event of a_i* (abbreviated by $i \rightarrow$).

Theorem 1. STICK_{AB} can be solved in $O(|A| + |B| + |E|)$ time.

Proof. Let $\sigma_A = (a_1, \dots, a_{|A|})$ and $\sigma_B = (b_1, \dots, b_{|B|})$. Let β_i denote the largest index such that b_{β_i} has a neighbor in a_1, \dots, a_i . Let \hat{B}^i be the elements of $(b_1, \dots, b_{\beta_i})$ that have a neighbor in $a_i, \dots, a_{|A|}$ ordered by σ_B , and let $\hat{B}^{i \rightarrow}$ be the elements of $(b_1, \dots, b_{\beta_i})$ that have a neighbor in $a_{i+1}, \dots, a_{|A|}$. At every event $p \in \{i, i \rightarrow\}$, we maintain the invariants that (i) we have a valid representation of the subgraph of G induced by $b_1, \dots, b_{\beta_i}, a_1, \dots, a_i$; (ii) for all these vertices,

their foot points are set as consecutive integers from 1 to $\beta_i + i$; and (iii) for those not in \hat{B}^p , their lengths are set.

Consider the enter event of a_i . We place a_i at position $\beta_i + i$. We place the vertices $b_{\beta_{i-1}+1}, \dots, b_{\beta_i}$ (if they exist) between a_{i-1} and a_i in this order and create \hat{B}^i by appending them to $\hat{B}^{(i-1)\rightarrow}$ in this order. All neighbors of a_i have to be before a_i , and they have to be a suffix of \hat{B}^i . This is easily checked in $\deg(a_i)$ time. The end point of a_i is placed directly above the foot point of its first neighbor in this suffix. As such, the invariants (i)–(iii) are maintained.

Consider the exit event of a_i and each neighbor b_j of a_i . If a_i is the last neighbor of b_j in σ_A , then we end b_j and set its endpoint at $\beta_i + i + 1/2$. We create $\hat{B}^{i\rightarrow}$ by removing each such b_j from \hat{B}^i . This again maintains invariants (i)–(iii). Hence, if we complete the exit event of $a_{|A|}$, we obtain a **STICK_{AB}** representation of G . Otherwise, G has no such representation. Clearly, the whole algorithm works in $O(|A| + |B| + |E|)$ time. Note that, even though we have not explicitly discussed isolated vertices, these are easily handled with length 0. \square

Theorem 2. *STICK_A* can be solved in $O(|A| \cdot |B|)$ time.

Proof. We assume that G is connected and discuss otherwise in Appendix A.

Overview. For each event $p \in \{i, i\rightarrow\}$, we maintain a data structure \mathcal{T}^p that compactly encodes all *realizable* permutations of certain horizontal sticks $B^p \subseteq B$. Namely, each B^i (resp. $B^{i\rightarrow}$) consists of all sticks of B with a neighbor in a_1, \dots, a_i and a neighbor in $a_i, \dots, a_{|A|}$ (resp. $a_{i+1}, \dots, a_{|A|}$). We denote by G^p the induced subgraph of G containing a_1, \dots, a_i and their neighbors. A permutation π of B^p is realizable if there is a stick representation of the graph obtained from G^p by adding a vertical stick to the right of a_i neighboring all horizontal sticks in B^p where B^p is drawn top-to-bottom in order π . In the enter event of a_i , we add to the data structure all the vertices of B that neighbor a_i and aren't in the data structure yet (we call these *entering vertices*), and constrain the data structure so that all the neighbors of a_i must occur after (below) the non-neighbors of a_i . In the exit event of a_i , we remove all sticks of B that do not have any neighbor a_j with $j > i$, i.e., they have a_i as their last neighbor (we call these *leaving vertices*). **Data structure.** See Fig. 1 for an example. Consider any event p . Observe that G^p may consist of several connected components $G_1^p, \dots, G_{k_p}^p$. Since G is connected, the components are naturally ordered from left to right by σ_A . Let B_j^p denote the vertices of B^p in G_j^p . In this case, in every realizable permutation of B^p , the vertices of B_j^p must come before the vertices of B_{j+1}^p . Furthermore, the vertices that will be introduced any time later can only be placed at the beginning, end, or between the components. Hence, to compactly encode the realizable permutations, it suffices to do so for each component G_j^p individually via a data structure T_i^p . Namely, our data structure will be $\mathcal{T}^p = (T_1^p, \dots, T_{k_p}^p)$.

Each data structure T_j^p is a rooted tree. At each node, its children consist of two types: the leaves (which correspond to the vertices of B_j^p) and the non-leaves. The non-leaves are ordered, while the leaves are unordered and can be placed anywhere before, after, or between the non-leaves with the same parent. A *valid*

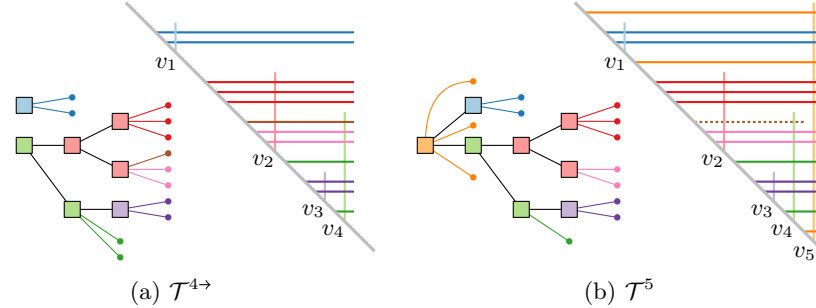


Fig. 1: An example for the data structure. In (b), the dotted stick has left the data structure and the leaves are permuted among the children to match the representation.

traversal of T_j^p is a pre-order traversal where, for each node, the non-leaf children are visited in the specified order and the leaves are permuted among the non-leaf children. Each permutation *expressed* by T_j^p corresponds to a valid traversal. Note that the non-leaves are visited in the same order in every valid traversal.

Correctness and event processing. We will argue that this data structure is sufficient to express the realizable permutations of B^p by induction. In the base case, consider the enter event of a_1 . Our data structure consists of a single component G_1^1 and clearly a single node with a leaf-child for every neighbor of a_1 captures all possible permutations.

Consider the exit event of a_i and assume that we have the data structure $\mathcal{T}^i = (T_1^i, \dots, T_{k_i}^i)$. If there are no leaving vertices, we just keep the data structures and are done. Otherwise, $B^{i\rightarrow}$ is a strict subset of B^i . We delete all leaves from \mathcal{T}^i corresponding to leaving vertices. If this results in any non-leaf node having only one child and that child is not a leaf, we merge it with its parent. If all children of an internal node get removed, we also remove the node. Obviously, this procedure maintains all realizable permutations of $B^{i\rightarrow}$ due to $G^{i\rightarrow}$.

Now consider the enter event of a_i and assume that we have the data structure $\mathcal{T}^{(i-1)\rightarrow} = (T_1^{(i-1)\rightarrow}, \dots, T_{k_{i-1}}^{(i-1)\rightarrow})$. The essential observation is that the neighbors of a_i must form a suffix of $B^{(i-1)\rightarrow}$ in every realizable permutation after the enter event, which we will enforce in the following. Namely, either

- all vertices in $B^{(i-1)\rightarrow}$ are adjacent to a_i ,
- none of them are adjacent to a_i , or
- there is an s such that (i) $B_s^{(i-1)\rightarrow}$ contains at least one neighbor of a_i ; (ii) all vertices in $B_{s+1}^{(i-1)\rightarrow}, \dots, B_{k_{i-1}}^{(i-1)\rightarrow}$ are neighbors of a_i ; and (iii) no vertices in $B_1^{(i-1)\rightarrow}, \dots, B_{s-1}^{(i-1)\rightarrow}$ are adjacent to a_i ; see Fig. 2a.

Otherwise, there is no realizable permutation for this event and consequently for G . The first two cases can be seen as degenerate cases (with $s = 0$ or $s = k_{i-1} + 1$) of the general case below.

We first show how to process $T_s^{(i-1)\rightarrow}$; see Fig. 2b. After that we will create the data structure \mathcal{T}^i . We create a tree T whose realizable permutations are

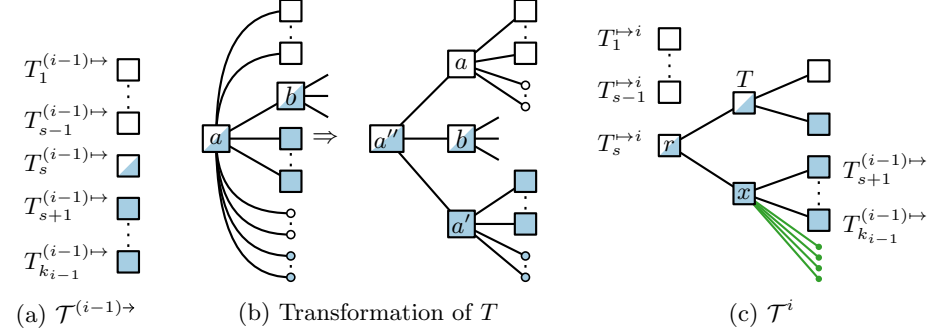


Fig. 2: Construction of \mathcal{T}^i . The leaves at the new node x are the entering vertices.

precisely the subset of those of $T_s^{(i-1) \rightarrow}$ where all leaves that are neighbors of a_i occur as a suffix. We initialize $T = T_s^{(i-1) \rightarrow}$. If all vertices in $B_s^{(i-1) \rightarrow}$ are neighbors of a_i , then we are already done.

Otherwise, we define a *marked* node as one where all leaves in its subtree are neighbors of a_i ; an *unmarked* node as one where no leaf in its induced subtree is a neighbor of a_i ; and a node is *half-marked* otherwise. Note that the root is half-marked. Since the neighbors of a_i must form a suffix, the marked non-leaf children of a half-marked node form a suffix, the unmarked non-leaf children form a prefix, and there is at most one half-mark child. Hence, the half-marked nodes form a path in T that starts in the root; otherwise, there are no realizable permutations for this event and subsequently for G .

We traverse the path leaf-to-root. Let a be a half-marked node, and let b be its half-marked child (if it exists). We have to enforce that in any valid traversal of T the unmarked children of a are visited before b and the marked children of a are visited after b . We create a new (marked) vertex a' and move all marked children of a to a' , preserving the order among the non-leaf children. Then we create a new (half-marked) node a'' and we hang a , b , and a' from a'' in this order. Finally, we put a'' into the former position of a in T . If this results in any internal node z with no leaf-children and only one child, we merge z with its parent. This ensures that all permutations realized by T have the neighbors of a_i as a suffix. Further, observe that the non-leaves of $T_s^{(i-1) \rightarrow}$ are visited in the same order in any valid traversal of T as in a valid traversal of $T_s^{(i-1) \rightarrow}$. The marked (unmarked) leaf-children of any half-marked node a of $T_s^{(i-1) \rightarrow}$ can be placed anywhere before, between, or after its marked (unmarked) children, but not before (after) b , since b has both marked and unmarked children. Hence, the permutations realized by T are exactly those realized by $T_s^{(i-1) \rightarrow}$ that have the neighbors of a_i as a suffix.

Now, we create the data structure \mathcal{T}^i ; see Fig. 2c. We set $T_1^i = T_1^{(i-1) \rightarrow}, \dots, T_{s-1}^i = T_{s-1}^{(i-1) \rightarrow}$. We additionally create T_s^i as follows. We hang $T_{s+1}^{(i-1) \rightarrow}, \dots, T_{k_{i-1}}^{(i-1) \rightarrow}$ from a new node x in this order. We further insert the entering vertices as leaf-

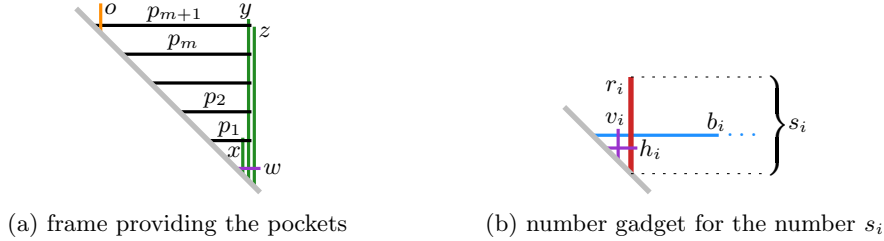


Fig. 3: Gadgets of our reduction from 3-PARTITION to STICK^{fix}.

children of x (note that this allows them to mix freely before, after, or between the components $G_{s+1}^{(i-1)\rightarrow}, \dots, G_{k_{i-1}}^{(i-1)\rightarrow}$. Then, we hang T followed by x off another node r , and make r the root of T_s^i . Finally, we set $\mathcal{T}^i = (T_1^i, \dots, T_s^i)$. This way, the order of the components $G_1^{(i-1)\rightarrow}, \dots, G_{k_{i-1}}^{(i-1)\rightarrow}$ of $G^{(i-1)\rightarrow}$ is maintained in the data structures for G^i . Furthermore, we ensure that the entering vertices can be placed exactly before, after, or between the components of $G^{(i-1)\rightarrow}$ that are completely adjacent to a_i . Hence, this data structure captures all realizable permutations of B^i due to G^i .

The decision problem of STICK_A can easily be solved by this algorithm. To find a stick representation, however, one has to backtrack through the data structures to find a valid permutation for the input problem. In Appendix A, we show how to do the backtracking and that the whole algorithm takes $O(|A||B|)$ time. \square

3 Sticks of Fixed Lengths

In this section, we consider the case that, for each vertex of the input graph, its stick length is part of the input and fixed. We denote the variants of this problem by STICK^{fix}, by STICK_A^{fix} if additionally σ_A is given, and by STICK_{AB}^{fix} if σ_A and σ_B given. Unlike the case with variable stick length, all three variants are NP-hard; see Sections 3.1 and 3.2. Surprisingly, STICK_{AB}^{fix} can be solved efficiently by a simple linear program if the input graph contains no isolated vertices (i.e., vertices of degree 0); see Section 3.3. With our linear program, we can check the feasibility of any instance of STICK^{fix} if we are given a total order of the sticks on the ground line. With our NP-hardness results, this implies NP-completeness.

3.1 STICK^{fix}

We show that STICK^{fix} is NP-hard by reduction from 3-PARTITION, which is strongly NP-complete [11]. In 3-PARTITION, one is given a multiset S of $3m$ integers s_1, \dots, s_{3m} such that, for $i \in \{1, \dots, 3m\}$, $C/4 < s_i < C/2$, where $C = (\sum_{i=1}^{3m} s_i)/m$, and the task is to decide whether S can be split into m sets of three integers, each summing up to C .

Theorem 3. STICK^{fix} is NP-complete.

Proof. We describe a polynomial-time reduction from 3-PARTITION. Given a 3-PARTITION instance $I = (S, C, m)$, we construct a fixed cage-like frame structure and introduce a number gadget for each number of S . A sketch of the frame is given in Fig. 3a. The purpose of the frame is to provide pockets, which will host our number gadgets (defined below). We add two long vertical (green) sticks y and z of length $mC + 1 + 2\varepsilon$ and a shorter vertical (green) stick x of length 1 that are all kept together by a short horizontal (violet) stick w of some length $\varepsilon \ll 1$. We use $m + 1$ horizontal (black) sticks p_1, p_2, \dots, p_{m+1} to separate the pockets. Each of them intersects y but not z and has a specific length such that the distance between two of these sticks is $C \pm \varepsilon$. Additionally, p_1 intersects x and p_{m+1} intersects a vertical (orange) stick o of length $2C$. We use x and o to prevent the number gadgets from being placed below the bottommost and above the topmost pocket, respectively. It does not matter on which side of y the stick x ends up since each b_i of a number gadget intersects y but neither x nor z .

For each number s_i in S , we construct a number gadget; see Fig. 3b. We introduce a vertical (red) stick r_i of length s_i . Intersecting r_i , we add a horizontal (blue) stick b_i of length at least $mC + 2$. The stick b_i intersects y and z , but neither x nor o . Due to these adjacencies, every number gadget can only be placed in one of the m pockets defined by p_1, \dots, p_{m+1} . It cannot span multiple pockets. We require that r_i and b_i intersect each other close to their foot points, so we introduce two short (violet) sticks h_i and v_i —one horizontal, the other vertical—of lengths ε ; they intersect each other, h_i intersects r_i , and v_i intersects b_i .

Given a yes-instance $I = (S, C, m)$ and a valid 3-partition P of S , the graph obtained by our reduction is realizable. Construct the frame as described before and place the number gadgets into the pockets according to P . Since the lengths of the three number gadgets' r_i sum up to $C \pm 3\varepsilon$, all three can be placed into one pocket. After distributing all number gadgets, we have a stick representation.

Given a stick representation of a graph G obtained from our reduction, we can obtain a valid solution of the corresponding 3-PARTITION instance $I = (S, C, m)$ as follows. Clearly, the shape of the frame is fixed, creating m pockets. Since the sticks b_1, \dots, b_{3m} are incident to y and z but neither to x nor to o , they can end up inside any of the pockets. In the y -dimension, each two number gadgets of numbers s_k and s_ℓ overlap at most on a section of length ε ; otherwise r_k and b_ℓ or r_ℓ and b_k would intersect. Each pocket hosts precisely three number gadgets: we have $3m$ number gadgets, m pockets, and no pocket can contain four (or more) number gadgets; otherwise, there would be a number gadget of height at most $(C + \varepsilon)/4 + 2\varepsilon$, contradicting the fact that s_i is an integer with $s_i > C/4$. In each pocket, the height of the number gadgets would be too large if the three corresponding numbers of S would sum up to $C + 1$ or more. Thus, the assignment of number gadgets to pockets defines a valid 3-partition of S . \square

The sticks of lengths s_1, \dots, s_{3m} can be simulated by paths of sticks with length ε each. Exploiting this, we can modify our reduction to use only three distinct stick lengths. We prove the following corollary in Appendix B.

Corollary 1. *STICK^{fix} with only three different stick lengths is NP-complete.*

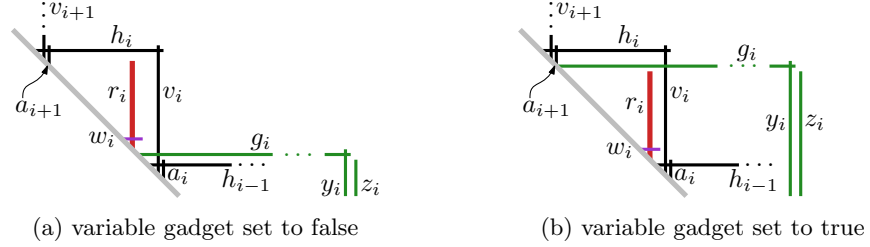


Fig. 4: Variable gadget in our reduction from MONOTONE-3-SAT to $\text{STICK}_A^{\text{fix}}$.

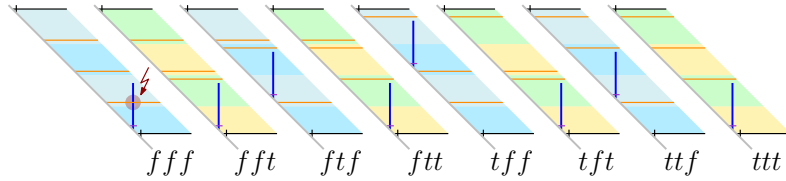


Fig. 5: Positive clause gadget (empty sub-stripe at the bottom). Here, a clause gadget for each of the eight possible truth assignments of a MONOTONE-3-SAT clause is depicted. E.g., tft means that the first variable is set to true, the second to false, and the third to true. Similarly, a negative clause gadget has an empty sub-stripe at the top.

3.2 $\text{STICK}_A^{\text{fix}}$ and $\text{STICK}_{AB}^{\text{fix}}$

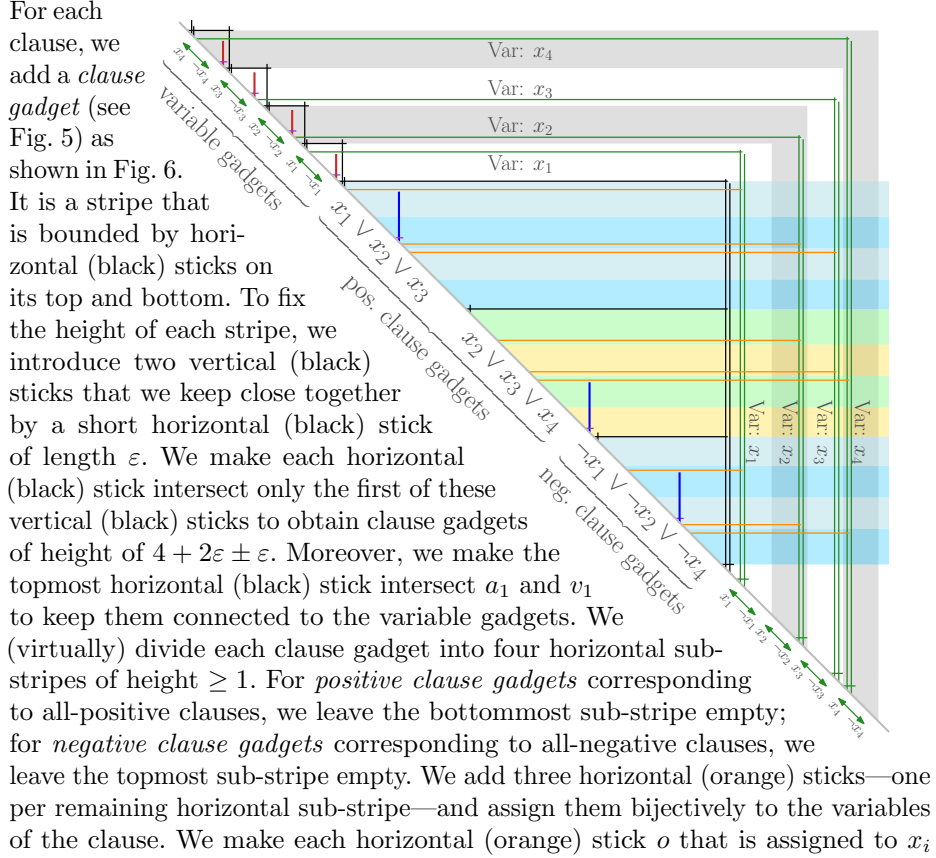
We show that $\text{STICK}_A^{\text{fix}}$ and $\text{STICK}_{AB}^{\text{fix}}$ are NP-hard by reduction from MONOTONE-3-SAT, which is NP-complete [20]. In MONOTONE-3-SAT, one is given a Boolean formula Φ in conjunctive normal form where each clause contains three distinct literals that are all positive or all negative. The task is to decide if Φ is satisfiable.

Theorem 4. $\text{STICK}_A^{\text{fix}}$ is NP-complete.

Proof. We describe a polynomial-time reduction from MONOTONE-3-SAT. A schematization of our reduction is depicted in Figs. 4 to 6. Given a MONOTONE-3-SAT instance Φ over variables x_1, \dots, x_n , we construct for each variable x_i (with $i \in \{1, \dots, n\}$) a *variable gadget* as depicted in Fig. 4. Inside a (black) cage, there is a vertical (red) stick r_i with length 1 and from inside, a long horizontal (green) stick g_i leaves this cage. We can enforce the structure to look like in Fig. 4 as follows. We prescribe the order σ_A of the vertical sticks as in Fig. 4. Since a_{i+1} has length $\varepsilon \ll 1$, the horizontal (black) stick h_i intersects the two vertical (black) sticks v_{i+1} and a_{i+1} close to its foot point. We have $\sigma_A(a_{i+1}) < \sigma_A(r_i) < \sigma_A(v_i)$, so r_i is inside the cage bounded by h_i and v_i and fixed its height—as it does not intersect h_i —making sticks h_i and v_i intersect close to their end points (both have length $1 + 2\varepsilon$). Moreover, r_i cannot be below h_{i-1} because a_i is shorter than r_i and intersects h_{i-1} to the right of r_i . The stick w_i intersects r_i close to r_i 's foot point because w_i has length ε . This leaves the freedom of placing g_i above or below r_i (as g_i does not intersect r_i) but still with its foot point inside the cage formed by h_i and v_i because it intersects v_i , but neither v_{i-1} nor v_{i+1} .

We say that the variable x_i is set to false if the foot point of g_i is below the foot point of r_i , and true otherwise. For each x_i , we add two long vertical (green) sticks y_i and z_i that we keep close together by a short horizontal (violet) stick of length ε (see Fig. 6 on the bottom right). We make g_i intersect y_i but not z_i . The three sticks g_i , y_i , and z_i get the same length ℓ_i . Hence, y_i and g_i intersect each other close to their end points as otherwise g_i would intersect z_i . We choose ℓ_1 sufficiently large such that the foot point of y_1 is to the right of the clause gadgets (see Fig. 6) and for each ℓ_i with $i \geq 2$, we set $\ell_i = \ell_{i-1} + 1 + 3\varepsilon$. Now compare the end points of g_i when x_i is set to false and when x_i is set to true relative to the (black) cage structure. When x_i is set to true, the end point of g_i is $1 \pm 2\varepsilon$ above and $1 \pm 2\varepsilon$ to the left compared to the case when x_i is set to false. Observe that, since g_i and y_i intersect each other close to their end points, this offset is also pushed to y_i and z_i and their foot points. Consequently, the position of the foot point of y_i (and z_i) differs by $1 \pm 2\varepsilon$ relative to the (black) frame structure depending on whether x_i is set to true or false. Our choice of ℓ_i allows this movement. In other words, no matter which truth value we assign to each x_i , there is a stick representation of the variable gadgets respecting σ_A .

Fig. 6: Illustration of our reduction from MONOTONE-3-SAT to STICK $_{\mathcal{A}}^{\text{fix}}$



intersect y_i and all y_j and z_j for $j < i$, but not z_i or y_k or z_k for any $k > i$. Thus, o intersects y_i close to o_i 's end points. We choose the length of each such o so that its foot point is at the bottom of its sub-stripe if x_i is set to false or is at the top of its sub-stripe if x_i is set to true. Within the positive and the negative clause gadgets, this gives us two times eight possible configurations of the orange sticks depending on the truth assignment of the three variables of the clause (see Fig. 5). Within each clause gadget, we have a vertical (blue) stick b of length 2. Each horizontal (black) stick that bounds a clause gadget intersects a short vertical (black) stick of length ε to force b into its designated clause gadget. Moreover, b is not isolated because it intersects a short (violet) stick of length ε .

Clearly, if Φ is satisfiable, there is a stick representation of the $\text{STICK}_A^{\text{fix}}$ instance obtained from Φ by our reduction by placing the sticks as described before (see also Fig. 6). In particular, the blue sticks can be placed as depicted in Fig. 5.

On the other hand, if there is a stick representation of the $\text{STICK}_A^{\text{fix}}$ instance obtained by our reduction, Φ is satisfiable. As argued before, the shape of the (black) frame structure of all gadgets is fixed by the choice of the adjacencies and lengths in the graph and σ_A . The only flexibility is, for each $i \in \{1, \dots, n\}$, whether g_i has its foot point above or below r_i . This enforces one of eight distinct configurations per clause gadget. As depicted in Fig. 5, precisely the configurations that correspond to satisfying truth assignments are realizable. Thus, we can read a satisfying truth assignment of Φ from the variable gadgets. \square

We enforce an order of the horizontal sticks except for a set W of sticks, which are the short (violet) sticks of length ε that are adjacent to the red and the blue sticks in the variable and clause gadgets. For STICK_{AB} we can prescribe σ_B if we remove the sticks W and use the same reduction to obtain Corollary 2. Observe that we now have isolated vertices (the red and blue vertical sticks).

Corollary 2. $\text{STICK}_{AB}^{\text{fix}}$ with isolated vertices in A or B is NP-complete.

3.3 $\text{STICK}_{AB}^{\text{fix}}$ without isolated vertices

In this section, we constructively show that $\text{STICK}^{\text{fix}}$ is efficiently solvable if we are given a total order of the vertices in $A \cup B$ on the ground line. Note that if there is a stick representation for an instance of STICK_{AB} (and consequently also $\text{STICK}_{AB}^{\text{fix}}$), the combinatorial order of the sticks on the ground line is always the same except for isolated vertices, which we formalize in the following lemma. The proof follows implicitly from the proof of Theorem 1. An explicit proof is given in the full version [8].

Lemma 1. *In all stick representations of an instance of STICK_{AB} , the order of the vertices $A \cup B$ on the ground line is the same after removing all isolated vertices. This order can be found in time $O(|E|)$.*

We are given an instance of $\text{STICK}^{\text{fix}}$ and a total order v_1, \dots, v_n of the vertices ($n = |A| + |B|$) with stick lengths ℓ_1, \dots, ℓ_n . We create a system of

difference constraints, that is, a linear program $Ax \leq b$ where each constraint is a simple linear inequality of the form $x_j - x_i \leq b_k$, with n variables and $m \leq 3n - 1$ constraints. Such a system can be modeled as a weighted graph with a vertex per variable x_i and a directed edge (x_i, x_j) with weight b_k per constraint. The system is solvable if and only if there is no directed cycle of negative weights, and a solution can be found in $O(nm)$ time with the Bellman–Ford algorithm.

For each stick v_i , we create a variable x_i that corresponds to the x-coordinate of v_i 's foot point on the ground line, with $x_1 = 0$. To ensure the unique order, we add $n - 1$ constraints $x_{i+1} - x_i \leq -\varepsilon$ for some suitably small ε and $i = 1, \dots, n - 1$.

Let $v_i \in A$ and $v_j \in B$. If $(v_i, v_j) \in E$, then the corresponding sticks have to intersect, which they do if and only if $x_j - x_i \leq \min\{\ell_i, \ell_j\}$. If $i < j$ and $(v_i, v_j) \notin E$, then the corresponding sticks must not intersect, so we require $x_j - x_i > \min\{\ell_i, \ell_j\} \geq \min\{\ell_i, \ell_j\} + \varepsilon$. This easily gives a system of difference constraints with $O(n^2)$ constraints. We argue that a linear number suffices.

Let $v_i \in A$. Let j be the largest j such that $(v_i, v_j) \in E$ and $\ell_j \geq \ell_i$. We add a constraint $x_j - x_i \leq \ell_i$. Further, let k be the smallest k such that $(v_i, v_k) \notin E$ and $\ell_k \geq \ell_i$. We add a constraint $x_k - x_i > \ell_i \Leftrightarrow x_i - x_k \leq -\ell_i - \varepsilon$. Symmetrically, let $v_i \in B$. Let j be the smallest j such that $(v_j, v_i) \in E$ and $\ell_j > \ell_i$. We add a constraint $x_i - x_j \leq \ell_i$. Further, let k be the largest k such that $(v_k, v_i) \notin E$ and $\ell_k > \ell_i$. We add a constraint $x_i - x_k > \ell_i \Leftrightarrow x_k - x_i \leq -\ell_i - \varepsilon$.

We now argue that these constraints are sufficient to ensure that G is represented by a solution of the system. Let $v_i \in A$ and $v_j \in B$. If $i > j$, then the corresponding sticks cannot intersect, which is ensured by the fixed order. So assume that $i < j$. If $\ell_j \geq \ell_i$ and $(v_i, v_j) \in E$, then we either have the constraint $x_j - x_i \leq \ell_i$, or we have a constraint $x_k - x_i \leq \ell_i$ with $i < j < k$; together with the order constraints, this ensure that $x_j - x_i \leq x_k - x_i \leq \ell_i$. If $\ell_j \geq \ell_i$ and $(v_i, v_j) \notin E$, then we either have the constraint $x_i - x_j \leq -\ell_i - \varepsilon$, or we have a constraint $x_i - x_k \leq -\ell_i - \varepsilon$ with $i < k < j$; together with the order constraints, this ensure that $x_i - x_j \leq x_i - x_k \leq -\ell_i - \varepsilon$. Symmetrically, the constraints are also sufficient for $\ell_j < \ell_i$. We obtain a system of difference constraints with n variables and at most $3n - 1$ constraints proving Theorem 5. By Lemma 1, there is at most one realizable order of vertices for a $\text{STICK}_{AB}^{\text{fix}}$ instance without isolated vertices, which can be found in linear time and proves Corollary 3.

Theorem 5. $\text{STICK}^{\text{fix}}$ can be solved in $O((|A| + |B|)^2)$ time if we are given a total order of the vertices.

Corollary 3. $\text{STICK}_{AB}^{\text{fix}}$ without isolated vertices is solvable in $O((|A| + |B|)^2)$ time.

4 Open Problems

We have shown that $\text{STICK}^{\text{fix}}$ is NP-complete even if the sticks have only three different lengths, while $\text{STICK}^{\text{fix}}$ for unit-length sticks is solvable in linear time. But what is the computational complexity of $\text{STICK}^{\text{fix}}$ for sticks with one of *two* lengths? Also, the three different lengths in our proof depend on the number of sticks. Is $\text{STICK}^{\text{fix}}$ still NP-complete if the fixed lengths are bounded? Beside this, the complexity of the original problem STICK is still open.

References

1. Cabello, S., Jejčič, M.: Refining the hierarchies of classes of geometric intersection graphs. *Electr. J. Comb.* **24**(1), P1.33 (2017), <http://www.combinatorics.org/ojs/index.php/eljc/article/view/v24i1p33>
2. Cardinal, J., Felsner, S., Miltzow, T., Tompkins, C., Vogtenhuber, B.: Intersection graphs of rays and grounded segments. *J. Graph Algorithms Appl.* **22**(2), 273–295 (2018). <https://doi.org/10.7155/jgaa.00470>
3. Catanzano, D., Chaplick, S., Felsner, S., Halldórsson, B.V., Halldórsson, M.M., Hixon, T., Stacho, J.: Max point-tolerance graphs. *Discrete Appl. Math.* **216**, 84–97 (2017). <https://doi.org/10.1016/j.dam.2015.08.019>
4. Chalopin, J., Gonçalves, D.: Every planar graph is the intersection graph of segments in the plane: Extended abstract. In: *STOC*. pp. 631–638. ACM (2009). <https://doi.org/10.1145/1536414.1536500>
5. Chaplick, S., Dorbec, P., Kratochvíl, J., Montassier, M., Stacho, J.: Contact representations of planar graphs: Extending a partial representation is hard. In: Kratsch, D., Todinca, I. (eds.) *WG. LNCS*, vol. 8747, pp. 139–151. Springer (2014). https://doi.org/10.1007/978-3-319-12340-0_12
6. Chaplick, S., Felsner, S., Hoffmann, U., Wiechert, V.: Grid intersection graphs and order dimension. *Order* **35**(2), 363–391 (2018). <https://doi.org/10.1007/s11083-017-9437-0>
7. Chaplick, S., Hell, P., Otachi, Y., Saitoh, T., Uehara, R.: Ferrers dimension of grid intersection graphs. *Discrete Appl. Math.* **216**, 130–135 (2017). <https://doi.org/10.1016/j.dam.2015.05.035>
8. Chaplick, S., Kindermann, P., Löffler, A., Thiele, F., Wolff, A., Zaft, A., Zink, J.: Stick graphs with length constraints. Arxiv report (2019), <http://arxiv.org/abs/1907.05257>
9. De Luca, F., Hossain, M.I., Kobourov, S.G., Lubiwi, A., Mondal, D.: Recognition and drawing of stick graphs. In: Biedl, T.C., Kerren, A. (eds.) *GD. LNCS*, vol. 11282, pp. 303–316. Springer (2018). https://doi.org/10.1007/978-3-030-04414-5_21
10. Felsner, S., Knauer, K.B., Mertzios, G.B., Ueckerdt, T.: Intersection graphs of L-shapes and segments in the plane. In: Csuha-J-Varijú, E., Dietzfelbinger, M., Ésik, Z. (eds.) *MFCS. LNCS*, vol. 8635, pp. 299–310. Springer (2014), some results herein are incomplete, see the warning on the full version: <http://page.math.tu-berlin.de/~felsner/Paper/dorgs.pdf>
11. Garey, M.R., Johnson, D.S.: *Computers and Intractability: A Guide to the Theory of NP-Completeness*. W. H. Freeman (1979)
12. Halldórsson, B.V., Aguiar, D., Tarpine, R., Istrail, S.: The Clark phaseable sample size problem: Long-range phasing and loss of heterozygosity in GWAS. *J. Comput. Biol.* **18**(3), 323–333 (2011). <https://doi.org/10.1089/cmb.2010.0288>
13. Hartman, I.B., Newman, I., Ziv, R.: On grid intersection graphs. *Discrete Math.* **87**(1), 41–52 (1991). [https://doi.org/10.1016/0012-365X\(91\)90069-E](https://doi.org/10.1016/0012-365X(91)90069-E)
14. Jünger, M., Leipert, S., Mutzel, P.: Level planarity testing in linear time. In: Whitesides, S.H. (ed.) *GD. LNCS*, vol. 1547, pp. 224–237. Springer (1998). https://doi.org/10.1007/3-540-37623-2_17
15. Klavík, P., Otachi, Y., Sejnoha, J.: On the classes of interval graphs of limited nesting and count of lengths. *Algorithmica* **81**(4), 1490–1511 (2019). <https://doi.org/10.1007/s00453-018-0481-y>
16. Köbler, J., Kuhnert, S., Watanabe, O.: Interval graph representation with given interval and intersection lengths. *J. Discrete Algorithms* **34**, 108–117 (2015). <https://doi.org/10.1016/j.jda.2015.05.011>

17. Kratochvíl, J.: A special planar satisfiability problem and a consequence of its NP-completeness. *Discrete Appl. Math.* **52**(3), 233–252 (1994). [https://doi.org/10.1016/0166-218X\(94\)90143-0](https://doi.org/10.1016/0166-218X(94)90143-0)
18. Kratochvíl, J., Matoušek, J.: Intersection graphs of segments. *J. Comb. Theory, Series B* **62**(2), 289–315 (1994). <https://doi.org/10.1006/jctb.1994.1071>
19. Kratsch, D., McConnell, R.M., Mehlhorn, K., Spinrad, J.P.: Certifying algorithms for recognizing interval graphs and permutation graphs. *SIAM J. Comput.* **36**(2), 326–353 (2006). <https://doi.org/10.1137/S0097539703437855>
20. Li, W.N.: Two-segmented channel routing is strong NP-complete. *Discrete Appl. Math.* **78**(1-3), 291–298 (1997). [https://doi.org/10.1016/S0166-218X\(97\)00020-6](https://doi.org/10.1016/S0166-218X(97)00020-6)
21. Lubiw, A.: Private communication (2019)
22. Matoušek, J.: Intersection graphs of segments and $\exists \mathbb{R}$. ArXiv, <https://arxiv.org/abs/1406.2636> (2014)
23. Pe'er, I., Shamir, R.: Realizing interval graphs with size and distance constraints. *SIAM J. Discrete Math.* **10**(4), 662–687 (1997). <https://doi.org/10.1137/S0895480196306373>
24. Schaefer, M.: Complexity of some geometric and topological problems. In: GD. LNCS, vol. 5849, pp. 334–344. Springer (2009). https://doi.org/10.1007/978-3-642-11805-0_32
25. Sen, M.K., Sanyal, B.K.: Indifference digraphs: A generalization of indifference graphs and semiorders. *SIAM J. Discrete Math.* **7**(2), 157–165 (1994). <https://doi.org/10.1137/S0895480190177145>
26. Shrestha, A.M.S., Takaoka, A., Tayu, S., Ueno, S.: On two problems of nano-PLA design. *IEICE Transactions* **94-D**(1), 35–41 (2011). <https://doi.org/10.1587/transinf.E94.D.35>
27. Spinrad, J., Brandstdt, A., Stewart, L.: Bipartite permutation graphs. *Discrete Appl. Math.* **18**(3), 279–292 (1987). [https://doi.org/10.1016/S0166-218X\(87\)80003-3](https://doi.org/10.1016/S0166-218X(87)80003-3)

Appendix

A Omitted proofs of Section 2

Theorem 2. STICK_A can be solved in $O(|A| \cdot |B|)$ time.

Proof (Continued). We continue the proof by first noting how one can handle disconnected graphs, and then discussing the backtracking and representation construction.

To handle disconnected graphs, we first identify the connected components H_1, \dots, H_t of G . We label each element of A by the index of the component to which it belongs. Now, observe that if σ_A contains a pattern of indices that alternate $abab$, then there can be no solution to STICK_A . Otherwise, we can treat each component separately by our algorithm, and then nest the resulting representations (whose construction we describe next via the backtracking) according to how the components nest in σ_A .

It remains to show how to do the backtracking and how to obtain the running time. The size of each data structure \mathcal{T}^p is in $O(|B^p|)$, since there are no degree-2 vertices in the trees and each leaf corresponds to a vertex in B . In each event, the transformations can clearly be done in time proportional to the size of the data structures. Since $|B^p| \leq |B|$ for each p and there are $2|A|$ events, the whole construction works in $O(|A||B|)$ time.

In the main text, we said that whenever a node x has exactly one child y and that child is an internal node, we merge x with its parent z . Instead of doing this, we will create a “shortcut” from y to z (and associate this shortcut with the last operation which caused x to be in this state). This way, we can traverse the tree without having to look at internal degree-2 nodes, but we keep them in the data structure for future reference. Also, we do not remove any leaves from the tree; we just mark them as *dead* and do not consider them anymore.

Assume that the algorithm processes all events without stopping. This means that, in every step, there was some realizable permutation. We now consider the data structure $\mathcal{T}^{|A| \rightarrow}$. Since we never actually removed anything but just marked leaves as dead and introduced shortcuts, removing the shortcuts and marking leaves as alive can be done in $O(|A||B|)$ time. This gives us a data structure \mathcal{T} that contains all vertices of B as leaves. In particular, \mathcal{T} gives us a permutation σ_B of B . Moreover, for every event p , σ_B restricted to B^p is a realizable permutation of B^p due to G^p . Thus, executing our algorithm for STICK_{AB} on σ_A and σ_B gives us a stick representation of G . \square

B Omitted proofs of Section 3

We modify the reduction used in the proof of Theorem 3 so that we use only three lengths. To this end, we use paths of sticks of length ε . We refer to them as ε -*paths*. Like a spring, an ε -path can be stretched (Fig. 7a) and compressed (Fig. 7c) up to a specific length. We will exploit the following properties regarding the minimum and the maximum size of an ε -path.

Lemma 2. *There is a stick representation of a $2n$ -vertex ε -path with height and width $n\varepsilon$ and another stick representation with height and width $\frac{n+2}{3}\varepsilon + \delta$ for any $\delta > 0$ and $n \geq 3$. Any stick representation of a $2n$ -vertex ε -path has height and width in the range $(\frac{n}{3}, n]\varepsilon$.*

Proof. We can arrange our sticks such that the foot points or the end points of two adjacent sticks touch each other (see Fig. 7a). This construction has height and width $n\varepsilon$ and, clearly, this is the maximum width and height for a $2n$ -vertex ε -path.

For the compressed ε -paths, we first describe a construction that has the specified width and height and, second, we show the lower bound.

The following construction is depicted in Fig. 7d for $n = 3$. Set the foot point of the first vertical stick in the path to $y = 0$ and the foot point of the third stick, which is also vertical, to $y = \varepsilon/3$. For each $i \in \{2, \dots, n-1\}$, set the foot point of the $(2i-2)$ -th stick (horizontal) to $y = i\varepsilon/3 + (i-2)\delta/(n-2)$ and the foot point of the $(2i+1)$ -th stick (vertical) to $y = i\varepsilon/3 + (i-1)\delta/(n-2)$. Set the foot point of the $(n-2)$ -th stick to $y = n\varepsilon/3 + \delta$, and the foot point of the last stick to $y = (n+1)\varepsilon/3 + \delta$. Observe that this construction has width and height $\frac{n+2}{3}\varepsilon + \delta$ and is a valid stick representation of a $2n$ -vertex ε -path.

Consider the i -th stick of an ε -path. On the one side of the line through this stick, there is the $(i-3)$ -th stick, and on the other, there is the $(i+3)$ -th stick. E.g., the second stick is to the right of the fifth stick and the eighth stick is to the left of the fifth stick. Since all sticks have length ε and non-adjacent sticks are not allowed to touch each other, the 1st, 4th, 7th, \dots , $(6k-2)$ -th stick for $k \in \mathbb{N}$ form a zigzag chain of width and height strictly greater than $k\varepsilon$. The same holds for the 2nd, 5th, \dots stick and the 3rd, 6th, \dots stick. Thus, for an ε -path of $2n$ sticks, we have width and height strictly greater than $\lceil \frac{2n}{6} \rceil \varepsilon \geq \frac{n}{3}\varepsilon$. \square

Corollary 1. *$\text{STICK}^{\text{fix}}$ with only three different stick lengths is NP-complete.*

Proof. We modify the reduction from 3-PARTITION to $\text{STICK}^{\text{fix}}$ described in the proof of Theorem 3 such that we use only three distinct stick lengths. We use the three lengths ε , Cm , and $3Cm$ (or longer, e.g. ∞). In Fig. 8, sticks of these lengths are violet, black, and green, respectively.

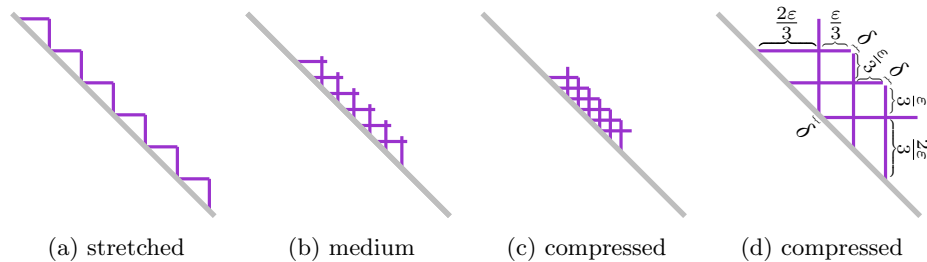


Fig. 7: An ε -path of 12 sticks in (a)–(c) and 6 sticks in (d).

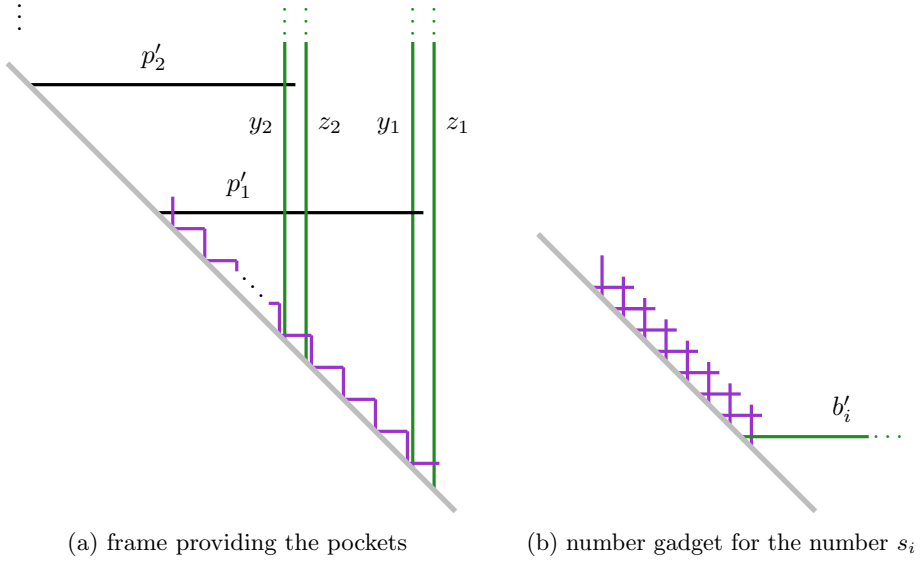


Fig. 8: Gadgets of our reduction from 3-PARTITION to STICK^{fix} with three stick lengths.

First, we describe the modifications of the frame structure, which are also depicted in Fig. 8a. Instead of the vertical (green) sticks x , y , and z used to fix all pockets, we have two vertical sticks y_j and z_j of length $3Cm$ for $j \in \{1, \dots, m+1\}$. Instead of the sticks p_1, \dots, p_{m+1} of different lengths, we use horizontal (black) sticks p'_1, \dots, p'_{m+1} each with length Cm to separate the pockets. The stick p'_j intersects y_k, z_k for all $k \in \{j+1, \dots, m+1\}$ and y_j but not z_j . All pairs y_j, z_j are kept together by a stick of length ε . For each two neighboring pairs y_j, z_j and y_{j+1}, z_{j+1} , these sticks of length ε are connected by an ε -path of $2C/\varepsilon$ sticks. According to Lemma 2, this effects a maximum distance of $(C/\varepsilon) \cdot \varepsilon \pm \varepsilon = C \pm \varepsilon$ between each two pairs of y_j, z_j and y_{j+1}, z_{j+1} . Accordingly, the pockets separated by the sticks p'_1, \dots, p'_{m+1} have height at most $C \pm 2\varepsilon$, similar as in the proof of Theorem 3. We keep the vertical (orange) stick o as in Figure 3a to prevent number gadgets from being placed above the topmost pocket, but now o has length $3Cm$.

Second, we describe the modifications of the number gadgets for each number s_i for $i \in \{1, \dots, 3m\}$, which are also depicted in Fig. 8b. We keep a long stick b'_i similar to b_i —now with length $3Cm$. We replace r_i (and h_i and v_i) by an ε -path of $6s_i/\varepsilon - 4$ sticks. We make the first stick of the ε -path intersect b'_i . By Lemma 2, this ε -path has a stick representation with height $s_i + \delta$ for any $\delta > 0$, but there is no stick representation with height $s_i - \frac{2}{3}\varepsilon$ or smaller. Clearly, these number gadgets can only be placed into one pocket since none of their sticks intersects a p'_j for $j \in \{1, \dots, m+1\}$.

Hence, we can represent a yes-instance of 3-PARTITION as such a stick graph if and only if the ε -paths of the number gadgets are (almost) as much compressed

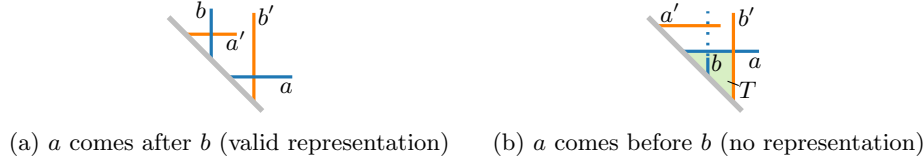


Fig. 9: Trying to represent a subgraph of the edges ab' and $a'b$ while respecting σ_A and σ_B .

as possible (to make the number gadgets small enough) and the ε -paths between the y_j - z_j sticks are (almost) as much stretched as possible (to make the pockets tall enough). Using this, the proof is the same as in Theorem 3. \square

Lemma 1. *In all stick representations of an instance of STICK_{AB} , the order of the vertices $A \cup B$ on the ground line is the same after removing all isolated vertices. This order can be found in time $O(|E|)$.*

Proof. Assume there are stick representations Γ_1 and Γ_2 of the same instance of STICK_{AB} without isolated vertices that have different combinatorial arrangements on the ground line. Without loss of generality, there is an $a \in A$ and a $b \in B$, such that in Γ_1 , a comes after b , while in Γ_2 , a comes before b (see Fig. 9). Clearly, a and b cannot be adjacent. Since a is not isolated, there is a b' that is adjacent to a and comes after b . Analogously, there is an a' that is adjacent to b and comes before a . In Γ_2 , a and b' define a triangle T (see Fig. 9b), which completely contains b since b occurs between a and b' , but is adjacent to neither of them. However, a' is outside of T as it comes before a . This contradicts b and a' being adjacent. The unique order can be determined in $O(|E|)$ time as described in Section 2. \square